Low band-gap polymers based on quinoxaline derivatives and fused thiophene as donor materials for high efficiency bulk-heterojunction photovoltaic cells

Jang-Yong Lee,[a] Won-Suk Shin,[b] Jung-Rim Haw[a] and Doo-Kyung Moon*[a]

Received 6th January 2009, Accepted 21st April 2009
First published as an Advance Article on the web 3rd June 2009
DOI: 10.1039/b823536h

In this study we synthesized three low band-gap polymers—poly[2,3-bis(4-hexyloxyphenyl)quinoxaline-alt-2,5-thieno[3,2-b]thiophene] (PQTT), poly[2,3-bis(4-hexyloxyphenyl)quinoxaline-alt-3,6-dipentadecylthieno[3,2-b]thiophene] (PQPDTT) and poly[2,3-bis(4-hexyloxyphenyl)quinoxaline-alt-2,5-bis(thieno-2-yl)-3,6-dipentadecylthieno[3,2-b]thiophene] (PQTPDTT)—that are based on quinoxaline and thieno[3,2-b]thiophene, and examined their photovoltaic properties. The band-gaps of PQTT and PQTPDTT were 1.65eV and 1.7eV, respectively. For PQTPDTT, a HOMO level of −5.12eV, which was lower than that of P3HT, was observed. According to the analysis of the characteristics of the photovoltaic device using $PC_{61}BM$ and $PC_{71}BM$ as acceptors, an open circuit voltage (V_{OC}) of 0.71V, a short circuit current (J_{SC}) of 8.80mA/cm^2, a fill factor of 0.36 and a power conversion efficiency (PCE) of 2.27% were observed at 100mW/cm^2 (AM 1.5 illumination) when a PQTPDTT/$PC_{71}BM$ blend film was used as the active layer. A very high incident photon to current efficiency (IPCE) was detected (60% at 400nm, 57% at 500nm).

Introduction

π-Conjugated polymers have been drawing great attention recently due to their application to related fields (*e.g.* OTFT, OLED, *etc.*),[1–4] their potential for fabricating low-cost integrated circuit elements for large areas and the feasibility of low-cost production using various methods such as spin coating, ink-jet printing and roll-to-roll through solution processes.[5–11] Thanks to the ease of cell production and efficient charge separation, bulk heterojunction-type organic solar cells, which contain a conjugated polymer and a fullerene as donor and acceptor, respectively, have been most widely studied out of the various organic solar cells.[12–17] In the beginning, the efficiency of organic solar cells was less than 1%. Since the adoption of fullerene as an acceptor, however, this figure has increased greatly. Due to a sharp advance in the field, devices reaching up to 5% in power conversion efficiency have recently been developed.[18–21] However, to achieve a 7% or higher level of power conversion efficiency, which is essential for the commercialization of organic solar cells, a variety of polymer materials that can overcome the existing limitations (stability, morphology, production techniques, *etc.*) must be developed.[22–24]

A high level (~5%) of PCE has been reported in polymer-based organic solar cells that use a regioregular poly(3-hexylthiophene) (P3HT) and [6,6]-phenyl C61 butyric acid methyl ester (PCBM) blend as the active layers.[25,26] Despite excellent charge transfer and separation, however, the polymer-based donor P3HT cannot absorb a wide range of photovoltaic power due to a relatively broad band-gap (1.9eV) and may lose much energy because of high LUMO levels.[27,28] As a result, it appears that the band-gap of bulk-heterojunction organic solar cells is optimum at 1.3–1.5eV with a LUMO level of 3.8eV, which is higher than that of an acceptor by 0.3–0.5eV.[29–33]

For the synthesis of lower band-gap polymers, many polymers have adopted an internal charge transfer between the electron-rich unit and the electron-deficient moiety.[34–36] It is regarded as a promising method for producing low band-gap polymers *via* which photons can be absorbed in a wide range of photovoltaic power, since alternating donor–acceptor units lower the effective band-gap by orbital mixing.

In this study, we synthesized new donor–acceptor-type low band-gap polymers—poly[2,3-bis(4-hexyloxyphenyl)quinoxaline-alt-2,5-thieno[3,2-b]thiophene] (PQTT), poly[2,3-bis(4-hexyloxyphenyl)quinoxaline-alt-3,6-dipentadecylthieno[3,2-b]thiophene] (PQPDTT) and poly[2,3-bis(4-hexyloxyphenyl)quinoxaline-alt-2,5-bis(thieno-2-yl)-3,6-dipentadecylthieno[3,2-b]thiophene] (PQTPDTT)—which contain quinoxaline (excellent electron-attraction unit) and thieno[3,2-b]thiophene, which has excellent planarity and abundant electrons. To improve the solubility of n-type materials and stabilize the excitons that are produced in molecules by the resonance effect, in particular, hexyloxybenzene was utilized. Furthermore, pentadecyl (a long alkyl chain) was used to increase the solubility of the fused thiophene. Bulk heterojunction-type devices with $PC_{61}BM$ and $PC_{71}BM$ as acceptors were fabricated in order to investigate the photovoltaic properties of PQTT, PQPDTT and PQTPDTT. Devices using the synthesized polymers and PCBM-blend films as active layers displayed a 1–2% power conversion efficiency. In those devices that used a PQTPDTT/$PC_{71}BM$ blend film, in particular, a very high level of PCE (2.27%) was detected (V_{OC} = 0.71V, J_{SC} = 8.80mA/cm^2, FF = 0.36). The process of the synthesis of monomers and polymers is shown in Scheme 1.

[a]*Department of Materials Chemistry and Engineering, Konkuk University, 1 Hwayang-dong, Gwangjin-Gu, Seoul, 143-701, South Korea. E-mail: dkmoon@konkuk.ac.kr; Fax: +82-2-444-0765; Tel: +82-2-450-3498*
[b]*Energy Materials Research Division, Korea Research Institute of Chemical Technology, P. O. BOX 107, Sinseongno 19, Yuseong, Daejeon, 305-600, South Korea. E-mail: shinws@krict.re.kr; Fax: +82-42-860-7868; Tel: +82-42-860-7106*

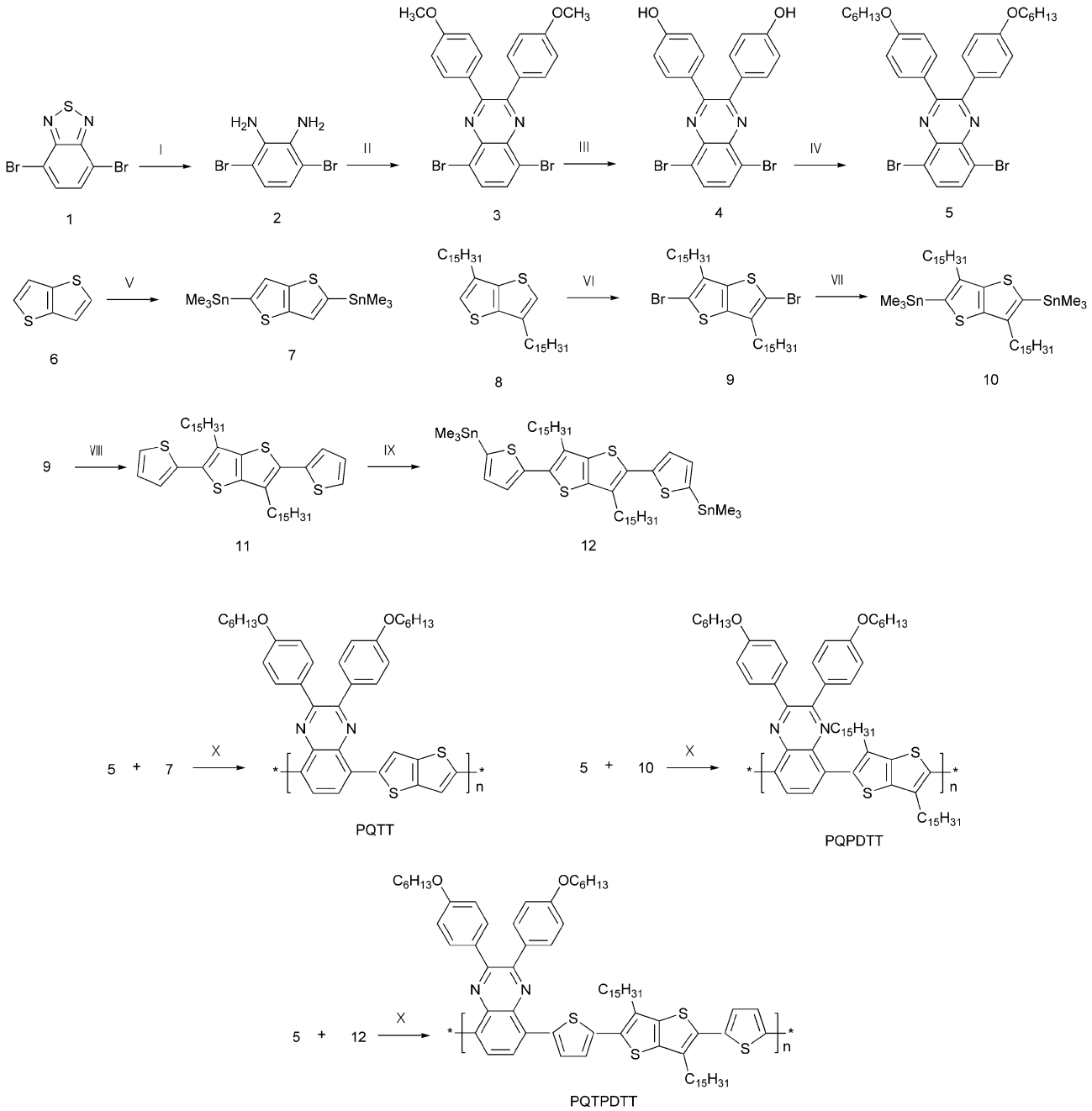

Scheme 1 The process of the synthesis of monomers and polymers. I) $NaBH_4$, ethanol; II) 4,4′-dimethoxybenzil, butanol; III) $C_5H_5N \cdot HCl$, reflux; IV) n-bromohexane, ethanol, reflux; V) THF, n-BuLi, Me_3SnCl, −50 °C; VI) CH_2Cl_2/AcOH, NBS; VII) THF, n-BuLi, Me_3SnCl; VIII) THF, 2-tributyltinthiophene, $Cl_2(PPh_3)_2Pd$; IX) THF, n-BuLi, Me_3SnCl; X) DMF/THF, $Cl_2(PPh_3)_2Pd$, reflux.

Results and discussion

To improve the solar absorption spectra and reduce the band-gap of polymers, thiophene and thieno[3,2-b]thiophene were used as electron donors and quinoxaline as an electron acceptor. Pentadecyl and hexyloxybenzene were attached to thieno[3,2-b]thiophene and quinoxaline respectively to increase solubility. Polymers were synthesized through a Stille coupling reaction, and low-molecular-weight materials were removed through reprecipitation and Soxhlet extraction of the solid product with methanol, acetone and hexane. The synthesis of polymers was investigated using ^{1}H-NMR, ^{13}C-NMR and elemental analysis. The synthesized polymers displayed high solubility in common organic solvents such as THF, chloroform, toluene, chlorobenzene and o-dichlorobenzene. Molecular weights were measured through GPC using THF as a solvent. According to these measurements, PQTT, PQPDTT and PQTPDTT had Mn values of 9 800, 8 668 and 14 065, Mw values of 14 600, 12 041 and 26 700, and PDIs of 1.44, 1.39 and 1.9, respectively.

Fig. 1 shows the UV-vis absorption spectra of polymers measured in the chloroform solution and in the film. For PQTT, the maximum absorption spectra were detected at 373nm and

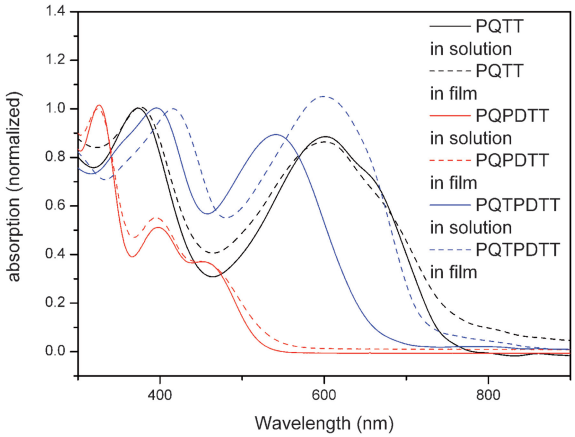

Fig. 1 UV-vis spectra of polymers in solution and in films.

597nm in solution and at 379nm and 598nm in the film. In contrast, the maximum absorption spectra were detected at 396nm and 540nm in solution and at 420nm and 600nm (about 60nm red-shifted) in the film for PQTPDTT. Similar results are often observed in polymers with an active inter-chain interaction. When compared to PQTT, PQTPDTT displayed greater 2D stacking in the film. Therefore, it appears that PQTPDTT is more effective than PQTT in shifting electrons and holes. Furthermore, PQTPDTT displayed better optical absorption within the range of 500–700nm, a range rich in photons, which

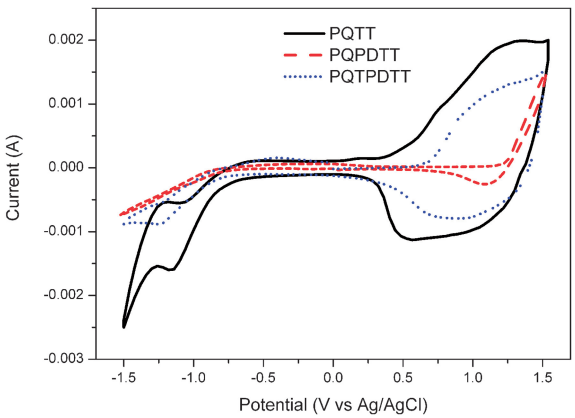

Fig. 2 Cyclic voltammograms of synthesized polymers.

means that PQTPDTT is more effective than PQTT in solar absorption with potential use as a polymer for organic solar cells. In terms of the optical band-gaps, which were measured through UV-vis absorption spectra, PQTT and PQTPDTT were 1.65eV and 1.7eV. For PQPDTT, however, the maximum absorption peaks were detected at 326nm, 397nm and 540nm (shoulder) in solution and there were no differences between the solution and the film. Furthermore, the UV-vis absorption spectra of PQPDTT were similar to those of quinoxaline derivatives. This indicates that there are no effective interactions between quinoxaline derivatives and fused thiophene derivatives. It is supposed to be caused by steric effects between long alkyl chains of quinoxaline derivatives and fused thiophenes.[37] The optical band-gap, which was calculated from the absorption onset, of PQPDTT was 2.3eV.

Fig. 2 shows the cyclic voltammograms of synthesized polymers. According to the analysis, PQTT and PQTPDTT were found to have oxidation potentials of 1.08V and 1.25V and reduction potentials of −1.3V and −1.23V. However, the oxidation and reduction potentials of PQPDTT were not clear. In contrast, the oxidation and reduction onset potentials of PQTT, PQPDTT and PQTPDTT were 0.52V, 1.21V and 0.68V, and −0.83V, −0.91V and −0.76V, respectively. As shown in Table 1, the HOMO and LUMO levels were −4.96eV and −3.61eV for PQTT, −5.6eV and −3.53eV for PQPDTT and −5.12eV and −3.68eV for PQTPDTT, respectively. Electrochemical band-gaps (which show the difference between the HOMO and LUMO levels) of 1.35eV (PQTT), 2.07eV (PQPDTT) and 1.44eV (PQTPDTT) were observed. Although all the polymers showed a small band-gap for the absorption of a wide range of photons, a high HOMO level was detected in PQTT, which implies poor oxidative stability due to a high HOMO level of thieno[3,2-b]thiophene (in polymers, an electron donor). Although the overall HOMO and LUMO energy levels decreased with the inclusion of an electron acceptor, the decrease in HOMO levels was not as great as the decrease in LUMO levels.[38] Conversely, compared to P3HT, PQTPDTT displayed excellent oxidative stability with a HOMO level of −5.12eV. Furthermore, a decrease in the LUMO level by intra-molecular interaction would be expected to improve the energy conversion efficiency by reducing energy loss.

The morphologies of the PCBM/polymer blend films were examined using AFM. The RMS thicknesses of PQTT/$PC_{61}BM$ and PQTT/$PC_{71}BM$ blend films (Fig. 3a and d) were relatively durable at 11.33nm and 25.45nm, respectively. It was also found

Table 1 The optical and electrochemical properties of polymers

	Absorption λ_{max} (nm)[a]			Energy level (eV)[d]			
Polymer	In solution	In film[b]	E_g^{op} (eV)[c]	HOMO	LUMO	E_g^{ec} (eV)[e]	$E_g^{op} - E_g^{ec}$ (eV)
PQTT	376, 598	378, 604	1.65	−4.96	−3.61	1.35	0.3
PQPDTT	326, 397, 540	325, 395, 540	2.3	−5.6	−3.53	2.07	0.23
PQTPDTT	398, 544	420, 600	1.7	−5.12	−3.68	1.44	0.26

All potentials are given vs. Ag/AgCl electrode.[a] λ_{max} was determined from UV-vis data. [b] Spin-coated from chloroform. [c] Estimated from the onset absorption of the thin film. [d] Calculated from the reduction and oxidation potentials under the assumption that the absolute energy level of Fc/Fc$^+$ was 4.8eV below a vacuum. [e] Band-gaps derived from the difference between onset potentials of oxidation and reduction.

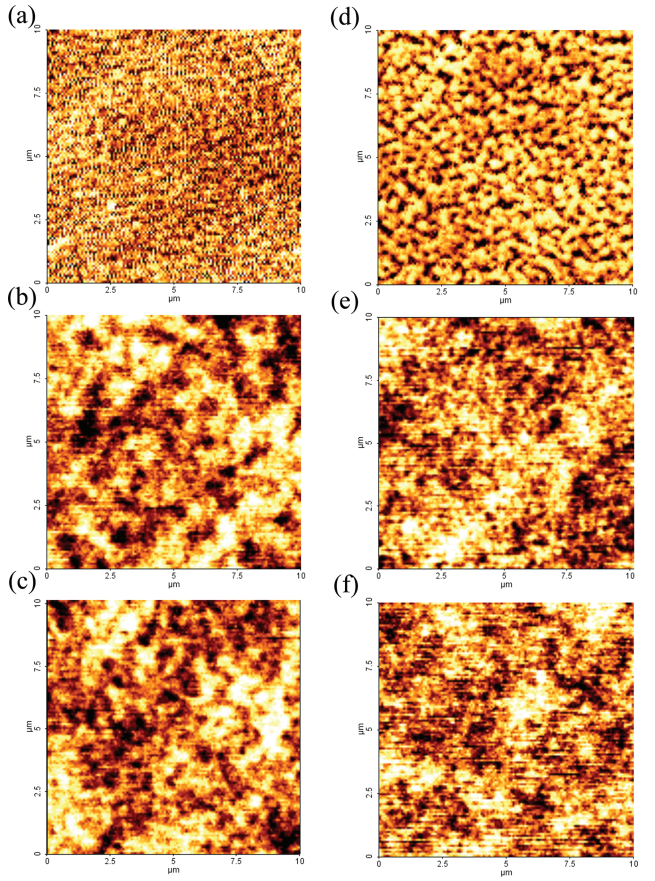

Fig. 3 AFM images of a) PQTT/$PC_{61}BM$, b) PQPDTT/$PC_{61}BM$, c) PQTPDTT/$PC_{61}BM$, d) PQTT/$PC_{71}BM$, e) PQPDTT/$PC_{71}BM$ and f) PQTPDTT/$PC_{71}BM$ blend films.

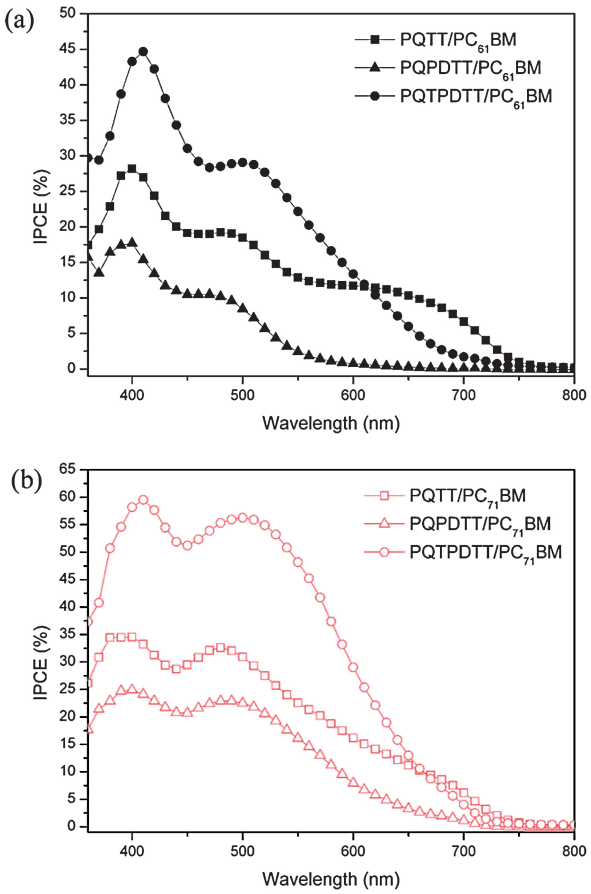

Fig. 4 Comparison of IPCE properties of the devices that have a) PQTT/$PC_{61}BM$, PQPDTT/$PC_{61}BM$ and PQTPDTT/$PC_{61}BM$, and b) PQTT /$PC_{71}BM$, PQPDTT/$PC_{71}BM$ and PQTPDTT/$PC_{71}BM$ blend films as active layers.

that polymer/PCBM films were poorly formed due to a local aggregation of PCBM. Conversely, the RMS thicknesses of PQPDTT/$PC_{61}BM$ and PQPDTT/$PC_{71}BM$ blend films (Fig. 3b and e) were 3.5nm and 3.4nm, and those of PQTPDTT/$PC_{61}BM$ and PQTPDTT/$PC_{71}BM$ blend films (Fig. 3c and f) were 3nm and 2.8nm. When compared to the film using PQTT as a donor, therefore, a far smoother morphology was observed. Although the channels of polymers and PCBM were not completely formed, charge transfer was smooth as the PCBM channels were, for the most part, well formed. It therefore appears that relatively good film properties were detected.[39] The optical and electrochemical properties of the polymers are summarized in Table 1.

Fig. 4 visually demonstrates the IPCE of polymer/PCBM bulk-heterojunction photovoltaic devices. In terms of IPCE, a clear difference was observed between the polymer/PCBM films depending on type. As shown in Fig. 4, PQTT/$PC_{61}BM$ and PQTPDTT/$PC_{61}BM$ films exhibited IPCE values of 27% and 45% at 400nm and 7–17% and 3–28% at 500nm–700nm, respectively. PQTT/$PC_{71}BM$ and PQTPDTT/$PC_{71}BM$ films also displayed high IPCEs at 400nm (35% and 60%). In contrast to the use of $PC_{61}BM$, high IPCE was observed at 500nm as well (33% and 57%). Although a decrease was detected at 500–700nm as with the introduction of $PC_{61}BM$, the IPCE almost doubled. This kind of change at 500nm occurred because the number of photons increased due to solar absorption by $PC_{71}BM$.[40] In comparison with PQTT and PQTPDTT, PQPDTT/PCBM films showed low IPCE values. This stems from poor absorption propertyies in the visible range of the spectrum.

Fig. 5 illustrates the I–V properties of fabricated devices. The thicknesses of active layers were adjusted with different spin coating conditions, and the devices were thermally treated at 120 °C before the LiF/Al electrodes were deposited thereon. The I–V curves of the organic solar cells show pronounced kinks.

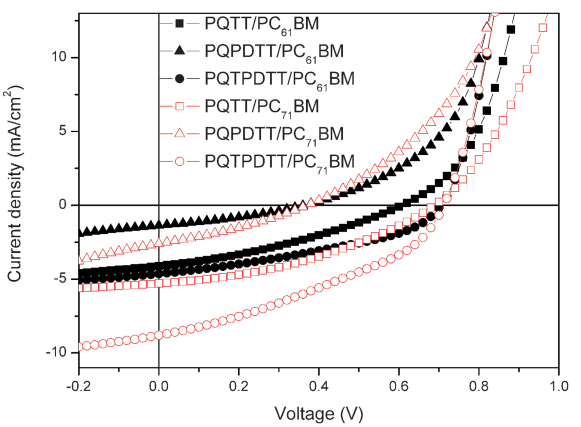

Fig. 5 Comparison of photovoltaic properties of the polymers.

Table 2 The photovoltaic properties of the devices[a]

Active layer	Layer thickness (nm)	V_{OC} (V)	J_{SC} (mA/cm^2)	FF	IPCE/λ (%/nm)	PCE (%)
PQTT/$PC_{61}BM$ = 1:3	60	0.61	4.12	0.33	28/400, 20/500	0.84
PQPDTT/$PC_{61}BM$ = 1:3	54	0.36	1.37	0.32	17/400, 10/470	0.16
PQTPDTT/$PC_{61}BM$ = 1:3	64	0.7	4.63	0.39	35/400, 33/500	1.28
PQTT/$PC_{71}BM$ = 1:3	50	0.69	5.29	0.38	45/420, 30/510	1.39
PQPDTT/$PC_{71}BM$ = 1:3	56	0.37	2.60	0.31	25/400, 23/500	0.30
PQTPDTT/$PC_{71}BM$ = 1:3	99	0.71	8.8	0.36	60/420, 56/510	2.27

[a] The measurements were carried out at 100mW/cm^2 (AM 1.5). The structure of the device was: ITO/PEDOT:PSS/polymer:PCBM/LiF/Al. Devices were annealed at 120 °C for 5 minutes before deposition of the LiF/Al electrode. Active area was 9mm^2 in all of the devices.

The peculiarity in the production of this device was the extremely fast evaporation rate of the top electrode. One might assume that there is some problem with the electrical properties of the top electrode. It would be one of factors which would substantially reduce the fill factor and therefore the photovoltaic performance.[41,42] As shown in Fig. 5, PQTT, PQPDTT and PQTPDTT exhibited V_{OC} of 0.61V, 0.36V and 0.7V, and J_{SC} values of 4.12mA/cm^2, 1.37mA/cm^2 and 4.63mA/cm^2, respectively, when $PC_{61}BM$ was used as an acceptor. When $PC_{71}BM$ was used, on the other hand, 0.69V, 0.37V and 0.71V V_{OC}, and 5.29mA/cm^2, 2.6mA/cm^2 and 8.8mA/cm^2 J_{SC} were observed. While no difference was detected in V_{OC}, there was a substantial difference in J_{SC} in both PQTT and PQTPDTT. This difference can be explained in terms of the results of IPCE in Fig. 4. In the case of PQTPDTT, in particular, a larger difference was observed in J_{SC} depending on the type of acceptor because IPCE was high even at 500–700nm. In terms of power conversion efficiency (PCE), the devices that used PQTT/$PC_{61}BM$, PQPDTT/$PC_{61}BM$ and PQTPDTT/$PC_{61}BM$ as active layers exhibited values of 0.84%, 0.16% and 1.28% while the devices that used PQTT/$PC_{71}BM$, PQPDTT/$PC_{71}BM$ and PQTPDTT/$PC_{71}BM$ as active layers gave values of 1.39%, 0.3% and 2.27%, respectively. The photovoltaic properties of the devices are summarized in Table 2.

Although V_{OC} and J_{SC} were high, complete efficiency was controlled by low fill factors. Low fill factors were apparently caused by poor morphology as in the results of AFM (Fig. 3). It appears that charge dissociation by poor morphology, decline in charge carrier transport and recombination of the electrons and holes would reduce fill factors. The morphology of a polymer/PCBM blend film could be improved by using various solvents at spin coating, changing the annealing temperature and adding various additives for better morphology. Due to the expansion of FF after the improved morphology, the properties of polymers could be greatly improved.

Experimental

Materials

All reagents and chemicals were purchased from Aldrich. Chloroform was dried over $CaCl_2$ and THF, toluene was dried over sodium under a nitrogen atmosphere. Other reagents and chemicals were used as received. 4,7-Dibromo-2,1,3-benzothiadiazole **1**,[43] 3,6-dibromo-1,2-phenylenediamine **2**,[44] thieno[3,2-b]thiophene **6**,[45,46] 3,6-dipentadecylthieno[3,2-b]thiophene **8**,[47] 2,5-dibromo-3,6-dipentadecylthieno[3,2-b]thiophene **9**[47] and 2,5-bis(2-thienyl)-3,6-dipentadecylthieno[3,2-b]thiophene **11**[47] were prepared as described in the literature.

Synthesis

2,3-Bis(4-methoxyphenyl)-5,8-dibromoquinoxaline 3. To a mixture of **2** (6g, 12.4mmol) and 4,4′-dimethoxybenzil (7.2g, 26.9mmol) in butanol (100ml), glacial acetic acid was added in several droplets, and then the solution was stirred at about 120 °C for 5 h. The solution was cooled to 0 °C and filtered. The separated solid was washed twice with hot ethanol and dried under vacuum oven to give a yellow solid (4g, 65%). Found: C, 52.68; H, 3.17; N, 5.6. $C_{22}H_{16}N_2O_2Br_2$ requires C, 52.76; H, 3.17; N, 5.6%; δ_H(400MHz; $CDCl_3$; Me_4Si) 3.85 (6H, s), 6.88 (4H, d, J = 8 Hz), 7.65 (4H, d, J = 8Hz), 7.85 (2H, s); δ_C(400MHz; $CDCl_3$; Me_4Si) 62.4, 114.6, 130.2, 132.9, 133.2, 142.2, 149.8, 157.3, 161.4.

2,3-Bis(4-hydroxyphenyl)-5,8-dibromoquinoxaline 4. In a two-neck-ed flask, **3** (4g, 8mmol) and pyridine hydrochloride (30eq) were added. After the mixture was stirred at 200 °C for 8 h, it was cooled to room temperature. Aqueous hydrochloric acid was poured into the mixture, and ether was added to extract the product from the aqueous layer. The organic layer was treated with dilute aqueous hydrochloric acid, aqueous sodium hydroxide and aqueous hydrochloric acid, in that order, and then further extracted with ether. The organic layer was washed with water and brine and dried over anhydrous Na_2SO_4. After the solvent was removed by rotary evaporation, the product was obtained as a yellow solid (3.58g, 95%). Found: C, 50.77; H, 2.55; N, 5.93. $C_{20}H_{12}N_2O_2Br_2$ requires C, 50.85; H, 2.54; N, 5.93%; δ_H(400MHz; $CDCl_3$; Me_4Si) 5.17 (2H, s), 6.82 (4H, d, J = 8 Hz,), 7.62 (4H, d, J = 8Hz), 7.85 (2H, s); δ_C(400MHz; $CDCl_3$; Me_4Si) 118.7, 130.2, 132.9, 133.2, 142.2, 149.8, 158.1, 169.1.

2,3-Bis(4-hexyloxyphenyl)-5,8-dibromoquinoxaline 5. To a solution of **4** (3.58g, 7.6mmol) in ethanol (50ml) was added aqueous potassium hydroxide (4eq). After the mixture was stirred for 1 h at room temperature, n-bromohexane was added. The reaction mixture was allowed to react at 70 °C for 24 h, then cooled to −20 °C. After filtration the crude product was purified by recrystallization from methanol to give a yellow solid (2.35g, 48%). Found: C, 59.88; H, 5.64; N, 4.33. $C_{32}H_{36}N_2O_2Br_2$ requires C, 59.97; H, 5.63; N, 4.38%; δ_H(400MHz; $CDCl_3$; Me_4Si) 0.91 (6H, t, J = 8Hz), 1.34 (8H, m, J = 4Hz), 1.48 (4H, m, J = 6Hz), 1.79 (4H, m, J = 6Hz), 3.99 (4H, t, J = 6Hz), 6.88 (4H, d, J = 8 Hz), 7.65 (4H, d, J = 8Hz), 7.85 (2H, s); δ_C(400MHz;

$CDCl_3$; Me_4Si) 14.5, 23.1, 29.6, 29.7, 30.1, 32.3, 68.8, 114.6, 130.2, 132.9, 133.2, 142.2, 149.8, 157.3, 160.4.

2,5-Bis(trimethylstannyl)thieno[3,2-b]thiophene 7. To a mixture of **6** (1 g, 7.13mmol) in anhydrous THF (50ml) was added a 2.5M solution of n-BuLi in hexane (6ml) at −50 °C under N_2. After 2h, a 1M solution of Me_3SnCl (15.7ml) in THF was added to the solution at −50 °C. After stirring at −50 °C for 2h, the solution was warmed to room temperature and stirred for 24h. The resulting mixture was poured into deionized water. $CHCl_3$ was added to extract the product from the aqueous layer, and the combined organic layers were washed with water and brine. The organic layer was dried over anhydrous Na_2SO_4, and the solvent was removed by rotary evaporation. The residue was purified by recrystallization from Et_2O to give colorless crystals (1.96g, 59%). Found: C, 57.12; H, 9.08; S, 7.23. $C_{12}H_{20}S_2Sn_2$ requires C, 56.93; H, 9.04; S, 7.23%; δ_H(400MHz; $CDCl_3$; Me_4Si) 0.38 (6H, s, J = 6.5 Hz), 7.25 (2H, s). δ_C(400MHz; $CDCl_3$; Me_4Si) −7.8, 126.5, 141.6, 147.9.

2,5-Bis(trimethylstannyl)-3,6-dipentadecylthieno[3,2-b]thiophene 10. To a mixture of **9** (3 g, 4.17mmol) in anhydrous THF (30ml) was added a 2.5M solution of n-BuLi in hexane (3.5ml) at −50 °C under N_2. After 2h, a 1M solution of Me_3SnCl (8.5ml) in THF was added to the solution at −50 °C. After stirring at −50 °C for 2h, the solution was warmed to room temperature and stirred for 24h. The resulting mixture was poured into a deionized water. $CHCl_3$ was added to extract the product from the aqueous layer, and the combinded organic layers were washed with water and brine. The organic layer was dried over anhydrous Na_2SO_4, and the solvent was removed by rotary evaporation. It was used directly in the next step without further purification. (2.88g, 78%). (Found: C, 57.43; H, 8.04; S, 12.18. $C_{42}H_{80}S_2Sn_2$ requires C, 57.18; H, 8.01; S, 12.2%) δ_H(400MHz; $CDCl_3$; Me_4Si) 0.38 (6H, s, J = 6.5 Hz), 7.25 (2H, s); δ_C(400MHz; $CDCl_3$; Me_4Si) -7.8, 14.4, 23.1, 29.1, 29.6, 31.5, 32.0, 32.1, 130.1, 132.7, 141.8.

2,5-Bis(5-trimethylstannyl-thienyl-2yl)-3,6-dipentadecylthieno[3,2-b]thiophene 12. To a mixture of 11 (1 g, 1.38mmol) in anhydrous THF (20mL) at −25 °C was added n-butyllithium (1.6M in hexane) by syringe. The mixture was stirred at −25 °C for 1h. Me_3SnCl was added dropwise to the solution, and the resulting mixture was warmed to room temperature and stirred for 24h. The mixture was poured into water and extracted with chloroform. The organic extracts were washed with brine and dried over anhydrous Na_2SO_4. The solvent was removed by rotary evaporation and the crude product was obtained as a yellow solid (0.57g, 40%). It was used directly in the next step without further purification. δ_H(400MHz; $CDCl_3$; Me_4Si) 7.34 (d, J = 4.9 Hz, 2H) 0.88 (6H, t, J = 6.5 Hz), 1.25–1.40 (48H, m), 1.76 (4H, m), 2.87 (4H, t, J = 7.9 Hz), 7.09 (2H, dd, J1 = 4.9 Hz, J2 = 2.6 Hz), 7.16 (2H, d, J = 2.6 Hz); δ_C(400MHz; $CDCl_3$; Me_4Si) −8.1, 14.4, 23.1, 29.1, 29.6, 31.5, 32.0, 32.1, 128.2, 129.6, 131, 133.3, 137.2, 140.9, 142.3.

General procedure of polymerization

To a mixture of $Pd(PPh_3)Cl_2$ (1.0 mol%) in DMF/THF (1/1) monomers were added. The mixture was vigorously stirred at 85–90 °C for 48h under nitrogen. After the mixture was cooled to room temperature, it was poured into methanol. A powder was obtained by filtration was reprecipitated with methanol several times. The polymer was further purified by washing with methanol, acetone and hexane, in a Soxhlet apparatus for 24h and dried under reduced pressure at 50 °C.

Poly[2,3-bis(4-hexyloxyphenyl)quinoxaline-alt-thieno[3,2-b]thiophene] (PQTT). Dark red solid (0.24g, 48.5%). Found: C, 73.42; H, 6.18; N, 4.53; S, 10.33; O, 5.32. $C_{38}H_{38}N_2S_2O_2$ requires C, 73.77; H, 6.19; N, 4.53; S, 10.34; O, 5.17%; T_g = 75 °C, T_m = 168 °C, T_d = 314 °C; δ_H(400MHz; $CDCl_3$; Me_4Si) 0.92 (6H, br), 1.37 (6H, br), 1.80 (4H, br), 3.95 (4H, br), 6.45 (4H, br), 6.9 (4H, br), 7.70 (4H, d); δ_C(400MHz; $CDCl_3$; Me_4Si) 14.4, 14.5, 23.0, 23.1, 26.1, 29.4, 29.6, 29.7, 29.9, 30.1, 32.0, 32.3, 68.4, 114.5, 130.9, 131.7, 132.1, 133.9, 139.1, 141.2, 147.1, 151.7, 156.3, 160.3.

Poly[2,3-bis(4-hexyloxyphenyl)quinoxaline-alt-3,6-dipentadecylthieno[3,2-b]thiophene] (PQPDTT). Red solid (0.11g, 22.2%). Found: C, 77.92; H, 9.46; N, 2.60; S, 6.22; O, 3.27. $C_{68}H_{98}N_2S_2O_2$ requires C, 78.57; H, 9.50; N, 2.69; S, 6.16; O, 3.08%; T_g = 49 °C, T_m = 141 °C, T_d = 298 °C; δ_H(400MHz; $CDCl_3$; Me_4Si) 0.78 (6H, br), 0.92 (6H, br), 1.14 (40H, br), 1.25 (6H, br), 1.36 (4H, br), 1.69 (4H, br), 1.81 (8H, br), 2.83 (4H, br), 3.87 (4H, br), 6.75 (4H, br), 7.57 (4H, br), 7.80 (2H, br); δ_C(400MHz; $CDCl_3$; Me_4Si) 14.4, 14.5, 23.0, 23.1, 26.1, 29.4, 29.6, 29.7, 29.9, 30.1, 32.0, 32.3, 68.4, 114.5, 130.9, 131.7, 132.1, 133.9, 139.1, 141.2, 147.1, 151.7, 156.3, 160.3.

Poly[2,3-bis(4-hexyloxyphenyl)quinoxaline-alt-2,5-bis(thieno-2-yl)-3,6-dipentadecylthieno[3,2-b]thiophene] (PQTDPT). Dark red solid (0.3g, 63.7%). Found: C, 75.14; H, 8.54; N, 2.20; S, 10.66; O, 2.68. $C_{76}H_{102}N_2S_4O_2$ requires C, 75.84; H, 8.54; N, 2.33; S, 10.64; O, 2.66%; T_g = 70 °C, T_m = 161 °C, T_d = 303 °C; δ_H(400MHz; $CDCl_3$; Me_4Si) 0.85 (6H, br), 0.92 (6H, br), 1.24 (40H, br), 1.35 (6H, br), 1.48 (4H, br), 1.56 (4H, br), 1.81 (8H, br), 3.0 (4H, br), 3.99 (4H, br), 6.88 (4H, br), 7.09 (2H, br), 7.6 (4H, br), 7.69 (2H, br), 7.91(2H, br); δ_C(400MHz; $CDCl_3$; Me_4Si) 14.4, 14.5, 23.0, 23.1, 26.1, 29.4, 29.6, 29.7, 29.9, 30.1, 32.0, 32.3, 68.4, 114.5, 130.9, 131.7, 132.1, 133.9, 139.1, 141.2, 147.1, 151.7, 156.3, 160.3.

Instruments

^{1}H-NMR and ^{13}C-NMR spectra were performed in a Brüker ARX 400 spectrometer using solutions in $CDCl_3$ and chemical shifts were recorded in ppm units with TMS as the internal standard. Elemental analyses were measured with EA1112 in a CE Instrument. The UV-vis spectra were measured with a HP Agilent 8453 UV-Vis. All GPC analyses were made using THF as eluent and polystyrene standard as reference. Cyclic voltammetric waves were produced by using a Wonatech WMPG 1000 with a 0.1 M acetonitrile (substituted a nitrogen in 20 min) solution containing tetrabutylammonium tetrafluoroborate ($TBABF_4$, Fluka 99.9%) at constant scan rate of 50 mV/s. A three-electrode cell was used and silver/silver chloride [Ag in 0.1M KCl] was used as a reference electrode. The luminance of devices was measured with a Spectra Scan PR-670. Current density-voltage (J-V) characteristics of all polymer photovoltaic cells were measured under the illumination of simulated solar light with 100 mW/cm^2 (AM 1.5 G) from an Oriel 1000W solar

simulator. Electric data were recorded using a Keithley 236 source-measure unit and all characterizations were carried out in the ambient atmosphere. The illumination intensity used was calibrated by a standard Si photodiode detector from Bunkoukeiki Co., Ltd. The incident photon-to-current conversion efficiency (IPCE) was measured as a function of wavelength from 360 to 800 nm (PV measurement Inc.) equipped with a halogen lamp as a light source, and calibration was performed using a silicon reference photodiode. Thicknesses of the thin films were measured using a KLA Tencor Alpha-step 500 surface profilometer with an accuracy of 1 nm.

Photovoltaic device fabrication

Composite solutions with polymers and PCBM were prepared using 1,2-dichlorobenzene (DCB). The concentration was controlled adequately in the range 1.0–2.0 wt%. For the measurement of optical absorption spectra of PCBM, the solutions were spun on pre-cleaned UV-grade silica substrates.

The polymer photovoltaic devices were fabricated with a typical sandwich structure of ITO/PEDOT:PSS/active layer/LiF/Al. The ITO coated glass substrates were cleaned through a routine cleaning procedure, including sonication in detergent followed by distilled water, acetone, and 2-propanol. A 45 nm thick layer of PEDOT:PSS (Baytron P) was spin coated on a cleaned ITO substrate after exposing the ITO surface to ozone for 10 min. The PEDOT:PSS layer was baked on a hot plate at 120 °C for 10 min. The active layer was spin-coated from the predissolved composite solution after filtering through 0.45 μm PP syringe filters. The device structure was completed by depositing a 200 nm Al cathode as the top electrode onto the polymer active layer under 3×10^{-6} torr vacuum in a thermal evaporator.

Conclusions

In this paper, quinoxaline-based poly[2,3-bis(4-hexyloxyphenyl)quinoxaline-alt-2,5-thieno[3,2-b]thiophene] (PQTT), poly[2,3-bis(4-hexyloxyphenyl)quinoxaline-alt-3,6-dipentadecylthieno[3,2-b]thiophene] (PQPDTT) and poly[2,3-bis(4-hexyloxyphenyl)quinoxaline-alt-2,5-bis(thieno-2-yl)-3,6-dipentadecylthieno[3,2-b]thiophene] (PQTPDTT) were successfully synthesized. PQTT and PQTPDTT showed low optical band-gaps of 1.65eV and 1.7eV. PQTPDTT, in particular, showed a greater solar absorption at 500–700nm, in which photons were abundant. However, PQPDTT had a comparatively high band-gap (2.3eV) and poor absorption spectra, because of an ineffective intramolecular interaction caused by steric effects between long alkyl chains of quinoxaline derivatives and fused thiophenes. In contrast to good morphology properties, it hindered PQPDTT to have a good photovoltaic properties. The device that used a PQTT/$PC_{71}BM$ blend film as an active layer had a power conversion efficiency (PCE) of 1.39% (V_{OC} = 0.69V, J_{SC} = 5.29mA/cm^2, FF = 0.38) while the device that contained a PQTPDTT/$PC_{71}BM$ blend film as an active layer reached up to 2.27% (V_{OC} = 0.71V, J_{SC} = 8.80mA/cm^2, FF = 0.36). Furthermore, according to the IPCE analysis, PQTPDTT had very high IPCE at 400nm (60%) and 500nm (57%). Therefore, it appears that PQTPDTT, which has excellent solar absorption and conversion properties, would have a better rate of PCE if studies on the improvement of morphology are continued to enhance the fill factor (FF).

Acknowledgements

This work was supported by the Korea Research Foundation Grant funded by the Korean Government (MOEHRD, Basic Research Promotion Fund) (KRF-2007-313-D00213). This work was supported by New & Renewable Energy R & D Program (2008-A011-0073) under the Korea Ministry of Knowledge Economy (MKE).

References

1 C. J. Yang, T. Y. Cho, C. L. Lin and C. C. Wu, *Appl. Phys. Lett.*, 2007, **90**, 173507.
2 S. H. Jin, H. J. Park, J. Y. Kim, K. Lee, S. P. Lee, D. K. Moon, H. J. Lee and Y. S. Gal, *Macromolecules*, 2002, **35**, 7532–7534.
3 T. Yasuda, T. Imase and T. Yamamoto, *Macromolecules*, 2005, **38**, 7378–7385.
4 J. Y. Lee, Y. J. Kwon, J. W. Woo and D. K. Moon, *J. Ind. Eng. Chem.*, 2008, **14**, 810–817.
5 F. C. Krebs, M. Jørgensen, K. Norrman, O. Hagemann, J. Alstrup, T. D. Nielsen, J. Fyenbo, K. Larsen and J. Kristensen, *Sol. Energy Mater. Sol. Cells*, 2009, **93**, 422–441.
6 F. C. Krebs, *Sol. Energy Mater. Sol. Cells*, 2009, **93**, 465–475.
7 M. Niggemann, B. Zimmermann, J. Haschke, M. Glatthaar and A. Gombert, *Thin Solid Films*, 2008, **516**, 7181–7187.
8 E. Bundgaard and F. C. Krebs, *Sol. Energy Mater. Sol. Cells*, 2007, **91**, 1019–1025.
9 C. Lungenschmied, G. Dennler, H. Neugebauer, S. N. Sariciftci, M. Glatthaar, T. Meyer and A. Meyer, *Sol. Energy Mater. Sol. Cells*, 2007, **91**, 379–384.
10 F. C. Krebs, H. Spanggard, T. Kjær, M. Biancardo and J. Alstrup, *Mater. Sci. En. B*, 2007, **138**, 106–111.
11 F. C. Krebs, J. Alstrup, H. Spanggaard, K. Larsen and E. Kold, *Sol. Energy Mater. Sol. Cells*, 2004, **83**, 293–300.
12 C. J. Brabec, N. S. Sariciftci and J. C. Hummelen, *Adv. Funct. Mater.*, 2001, **11**, 12–26.
13 H. Hoppe and N. S. Sariciftci, *J. Mater. Res.*, 2004, **19**, 1924–1945.
14 K. M. Coakley and M. D. McGehee, *Chem. Mater.*, 2004, **16**, 4533–4542.
15 S. Gunes, H. Neugebauer and N. S. Sariciftci, *Chem. Rev.*, 2007, **107**, 1324–1338.
16 C. Winder and N. S. Saridifti, *J. Mater. Chem.*, 2004, **14**, 1077–1082.
17 J. Li, F. Dierschke, J. Wu, A. C. Grimsdale and K. Müllen, *J. Mater. Chem.*, 2006, **16**, 96–102.
18 J. Peet, J. Y. Kim, N. E. Coates, W. L. Ma, D. Moses, A. J. Heeger and G. C. Bazan, *Nat. Mater.*, 2007, **6**, 497–500.
19 E. Wang, L. Wang, L. Lan, L. Luo, W. Zhuang, J. Peng and Y. Cao, *Appl. Phys. Lett.*, 2008, **92**, 033307.
20 L. H. Slooff, S. C. Veenstra, J. M. Kroon, D. J. D. Moet, J. Sweelssen and M. M. Koetse, *Appl. Phys. Lett.*, 2007, **90**, 143506.
21 N. Blouin, A. Michaud and M. Leclerc, *Adv. Mater.*, 2007, **19**, 2295–2300.
22 I. B. Zimmermann, U. Wűrfel and M. Niggemann, *Sol. Energy Mater. Sol. Cells*, 2009, **93**, 491–496.
23 M. Jørgensen, K. Norrman and F. C. Krebs, *Sol. Energy Mater. Sol. Cells*, 2008, **92**, 686–714.
24 B. C. Thompson and J. M. J. Fréchet, *Angew. Chem. Int. Ed.*, 2008, **47**, 58–77.
25 W. Ma, C. Yang, X. Gong, K. Lee and A. J. Heeger, *Adv. Funct. Mater.*, 2005, **15**, 1617–1622.
26 G. Li, V. Shrotriya, J. Huang, Y. Yao, T. Moriarty, K. Emery and Y. Yang, *Nat. Mater.*, 2005, **4**, 864–868.
27 E. Bundgaard and F. C. Krebs, *Sol. Energy Mater. Sol. Cells*, 2007, **91**, 954–985.
28 R. Kroon, M. Lenes, J. C. Hummelen, P. W. M. Blom and B. De Boer, *Polym. Rev.*, 2008, **48**, 531–582.

29 S. A. Choulis, J. Nelson, Y. Kim, D. Poplavskyy, T. Kreouzis, J. R. Durrant and D. D. C. Bradley, *Appl. Phys. Lett.*, 2003, **83**, 3812–3814.
30 V. D. Mihailetchi, J. K. V. Duren, P. W. M. Blom, J. C. Hummelen, R. A. J. Janssen, J. M. Kroon, M. T. Rispens, W. J. H. Verhees and M. M. Wienk, *Adv. Funct. Mater.*, 2003, **13**, 43–46.
31 B. C. Thompson, Y. G. Kim and J. R. Reynolds, *Macromolecules*, 2005, **38**, 5359–5362.
32 M. C. Scharber, D. Mühlbacher, M. Koppe, P. Denk, C. Waldauf, A. J. Heeger and C. J. Brabec, *Adv. Mater.*, 2006, **18**, 789–794.
33 L. J. A. Koster, V. D. Mihailetchi and P. W. M. Blom, *Appl. Phys. Lett.*, 2006, **88**, 093511–3.
34 E. Bundgaard, S. E. Shaheen, F. C. Krebs and D. S. Ginley, *Sol. Energy Mater. Sol. Cells*, 2007, **91**, 1631–1637.
35 E. Bundgaard and F. C. Krebs, *Sol. Energy Mater. Sol. Cells*, 2007, **91**, 954–985.
36 E. Bundgaard and F. C. Krebs, *Macromolecules*, 2006, **39**, 2823–2831.
37 X. Zhang, M. Khler and A. J. Matzger, *Macromolecules*, 2004, **37**, 6306–6315.
38 A. R. Murphy, J. Liu, C. Luscombe, D. Kavulak, J. M. J. Frechet, R. J. Kline and M. D. McGehee, *Chem. Mater.*, 2005, **17**, 4892–4899.
39 A. J. Moule, A. Tsami, T. W. Bunnagel, M. Forster, N. M. Kronenberg, M. Scharber, M. Koppe, M. Morana, C. J. Brabec, K. Meerholz and U. Scherf, *Chem. Mater.*, 2008, **20**, 4045–4050.
40 D. Muhlbacher, M. Scharber, M. Morana, Z. Zhu, D. Waller, R. Gaudiana and C. Brabec, *Adv. Mater.*, 2006, **18**, 2884–2889.
41 M. Glatthaar, M. Riede, N. Keegan, K. Sylvester-Hvid, B. Zimmermann, M. Niggemann, A. Hinsch and A. Gombert, *Sol. Energy Mater. Sol. Cells*, 2007, **91**, 390–393.
42 S. T. Zhang, Y. C. Zhou, J. M. Zhao, Y. Q. Zhan, Z. J. Wang, Y. Wu, X. M. Ding and X. Y. Hou, *Appl. Phys. Lett.*, 2006, **89**, 043502.
43 X. Li, W. Zeng, Y. Zhang, Q. Hou, W. Yang and Y. Cao, *Eur. Polym. J.*, 2005, **41**, 2923–2933.
44 R. Yang, R. Tian, J. Yan, Y. Zhang, J. Yang, Q. Hou, W. Yang, C. Zhang and Y. Cao, *Macromolecules*, 2005, **38**, 244–253.
45 L. S. Fuller, B. Iddon and K. A. Smith, *J. Chem. Soc., Perkin Trans. 1*, 1997, 3465–3470.
46 H. S. Kim, Y. H. Kim, T. H. Kim, Y. Y. Noh, S. Pyo, M. H. Yi, D. Y. Kim and S. K. Kwon, *Chem. Mater.*, 2007, **19**, 3561–3567.
47 Y. Li, Y. Wu, P. Liu, M. Birau, H. Pan and B. S. Ong, *Adv. Mater.*, 2006, **18**, 3029–3032.